Evidence for discrete cell kinetic subpopulations in mouse epidermis based on mathematical analysis

C. S. Potten, H. E. Wichmann*, M. Loeffler*, K. Dobek* and D. Major†

Paterson Laboratories, and †Medical Physics, Christie Hospital, Manchester, England, and *Medizinische Universitätsklinik Köln, Germany

Abstract. Continuous (repeated) labelling studies in mouse epidermis indicate that nearly all cells are labelled after about 100 hr. Percentage labelled mitoses studies ([³H]TdR at 15.00 and 03.00 hours) have a first peak that does not reach 100% and has a half-width of about 10 hr. Small second and third peaks can be detected at about 90 and 180 hr, respectively. The changes with time in the number of labelled cells show a difference dependent on the time of day of [³H]TdR administration. Both curves show an early doubling in labelled cells which then decline, forming a peak of labelled cells. A second peak occurs at about 120 hr. This is followed by a progressive decline with no further peaks until values of about 1% labelling are obtained at 340 hr.

These experiments have been investigated mathematically. A computer programme has been devized that permits all three types of experiments to be analysed simultaneously. More importantly, it can analyse situations with a heterogeneity in cell cycle parameters in all proliferative subpopulations.

Various models for epidermal cell replacement have been considered. The data as a whole can best be explained if the basal layer contains at least two distinct subpopulations of cells and an exponentially decaying post-mitotic population with a half-life of about 30 hr. The proliferative sub-populations must be characterized by near integer differences in the length of cycle, the precursor (stem) compartment having the longer cycle. An inverse relationship is required for the length of S, i.e. the shortest time for the stem cells.

A full range of cell kinetic parameters can be calculated and are tabulated for the most appropriate model system which is one involving three transit proliferating subpopulations.

There is a fairly extensive literature on the cell kinetics of mouse skin under 'steady state' conditions; most reports, however, provide rather limited information such as simple indices for the fraction of cells in mitosis (M) or DNA synthesis (S). These data have been reviewed in the past (Potten, 1975a) and some aspects have been reconsidered recently (Potten, 1980). When the marked circadian rhythm (e.g. see Tvermyr, 1969, 1972) is taken into account the data suggest that the epidermis from mouse dorsum has an average cell cycle time (T_C) that is poorly defined, but probably lies between 100 and 200 hr. The duration of the S phase (T_S) is

Correspondence: Dr C. S. Potten, Paterson Laboratories, Christie Hospital, Manchester M20 9BX, England.

better defined lasting about 11 hr, while the duration of M (T_M) is probably between 1·0 and 1·5 hr. T_{G_2} is poorly defined, probably less than 15 hr. Some of the variability in these cell kinetic parameters is undoubtedly due to differences inherent in the various mouse strains studied and to the use of different assay techniques.

Some clonal regeneration studies suggested that only 2–7% of the basal cells were clonogenic (Potten & Hendry, 1973). These estimates have inherently large errors. Recent studies have suggested that the epidermis is, in fact, subdivided into discrete functional cell groupings, called epidermal proliferative units (EPUs) (Potten, 1974) which, because of their size, suggest that the clonogenic fraction (stem cell fraction) is probably in fact about 9%, i.e. 1 in 10·6 (the total basal cell complement of an EPU). In all cell kinetic studies in skin it should be noted that 12–15% of the basal cells are in fact 'clear cells'; Langerhans, indeterminate and pigment cells (Allen & Potten, 1974). These do not contribute to keratinocyte replacement but are included in the average value of 10·6 cells per EPU. If they are excluded then the clonogenic cells would comprise about 10·8% of the basal layer keratoblasts.

Cell replacement in epidermis could theoretically be explained by two basic models (first outlined by Gilbert & Lajtha, 1965); firstly it could be achieved by cell division in a proliferatively homogenous basal layer where all the proliferating cells are stem cells ('A' cells in Fig. 1). This type of model has been assumed by many workers in the past. On the other hand, part of the cell replacement could be achieved by cell division in a second transitory proliferating cell population ('T' or transit, cells in models 3–5 in Fig. 1, each T population representing one cell cycle).

In this paper we wish to consider mathematically and experimentally three different cell kinetic experiments conducted on the same strain, sex and age of mouse in the light of the models outlined in Fig. 1. The purpose is to see whether or not models involving a proliferatively homogenous basal layer can be rejected on cell kinetic grounds as well as on the basis of the clonal regeneration studies, or whether any alternative models could be envisaged.
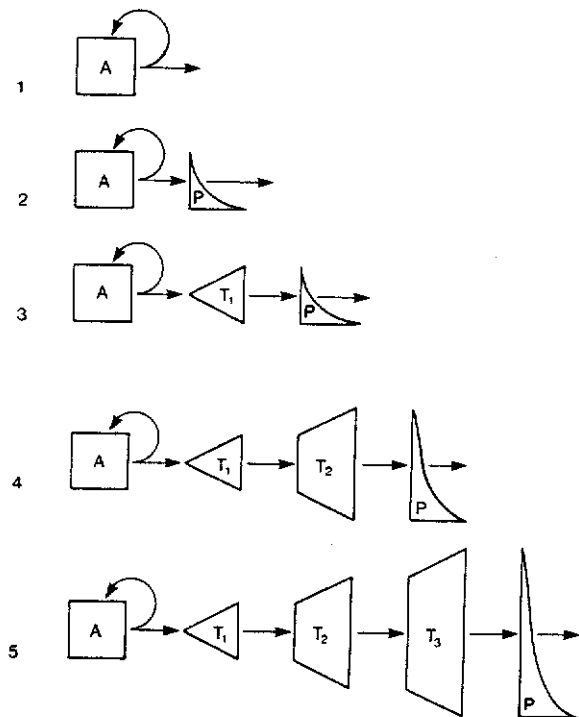

Fig. 1. Five possible models to explain cell replacement in epidermis under steady state conditions are shown. The models and the terminology used are based on that described by Gilbert & Lajtha (1965). Three major sub-classes of cells can be defined: stem cells, A; transitory proliferating cells of which there are three in this diagram, T_1, T_2 and T_3 (each representing one cell cycle), and post-mitotic maturing cells P. An exponential loss out of the basal layer is assumed for the P compartment. Further models with T_4 and T_5 populations could also be considered as generalizations of model 5.

MATERIALS AND METHODS

Experimental

Three experiments are to be considered here. One of these, namely a continuous labelling experiment (CL), has been presented elsewhere (Potten, Kovacs & Hamilton, 1974; Potten & Major, 1980). The other two experiments, a percentage labelled mitoses study (PLM) and a study on the changes in labelling index (LI) with time after a single injection of [³H]TdR, will eventually be published in greater detail.

For all the experiments male DBA2/J mice between the ages of 7 and 8 weeks were used. Mice of this age and sex have their hair growth cycle synchronized in the resting phase. They were caged in groups of four and held in rooms where the light, temperature and humidity were controlled and noise and external disturbance were kept to a minimum. The animals were allowed a minimum of 4 weeks to acclimatize to these conditions before their use in any experiment. The mice were injected with 25 μCi [³H]TdR (5 Ci/mM) at either 03.00 or 15.00 hours (12.00 hours for some of the CL experiments), and were killed in groups of four to six animals at various times thereafter. Parts of the experiment were repeated several times and the results of these were eventually pooled so that, for some sample times, up to sixteen mice were used.

Sections (PLM) or epidermal sheet preparations (LI) were dipped in Ilford K5 emulsion and exposed for 10–21 days (PLM) or 4–6 weeks (LI). A minimum total of 100 mitoses from slides from four mice were scored for the PLM experiment using a grain count threshold of 2–3 grains. The lower threshold, when applied to slides exposed for 10 days, was considered, after empirical observations, to be roughly equivalent to the higher threshold for slides exposed for 21 days. A minimum of 1000 basal cells were scored per mouse for the LI experiment using four different areas on epidermal sheets.

Samples were taken in each experiment for times up to about 200 hr (340 hr in the LI experiment) and, since the same animals were studied for some of the experiments, the results could be directly inter-related and compared with theoretical curves generated for the three experiments, using various models.

Mathematical approach

A total of five possible models was considered. These were formulated mathematically and theoretical LI, PLM and CL curves were calculated. These were then compared with the actual experimental results. A computer program was developed which can analyse all three types of experiment simultaneously. Uniquely, it can consider situations with a heterogeneity in the proliferative compartments (see appendix). In order to compute the theoretical curves, assumptions had to be made about certain cell cycle parameters. It was assumed that as a starting point T_C must lie between about 100 and 200 hr. The average value assumed for T_S was within 8–14 hr; T_{G_2} was assumed to be between 2·5 and 5 hr while T_M was within the range 0·5–2 hr. The average residence time (T_p) in the basal layer for a post-mitotic maturing cell (P) was assumed to be 45 hr, giving a 'half-life' in the basal layer of about 30 hr, assuming a random loss. One further assumption was that 15% of the basal cells are 'clear' cells which do not contribute proliferatively. We assume, except for model 1, that there is no loss from any compartment except P. Biologically this means that most mitoses are in a plane parallel to the basement membrane and for simplicity the number of vertical mitoses was assumed to be negligible. The mathematical methods are presented in the appendix.

RESULTS

Experimental results

Figure 2 shows the changes in LI with time after a single injection of [³H]TdR at 03.00 hours. The initial labelling index is 6·7%. Two hours later a lower LI is obtained. Then the curve rises and a value double the initial LI is obtained by 12 hr. There is then an apparent continued rise to LI values of about 15%. These elevated LI values persist for about 40 hr and then, by about 90 hr, fall to reach a minimum about 1·5 times the initial LI. There is a subsequent return to LI values that are double the initial LI at about 115 hr. The LI then decays steadily until it reaches its initial value at about 190 hr and about 1% LI at 336 hr. No clear evidence of a third peak can be detected.
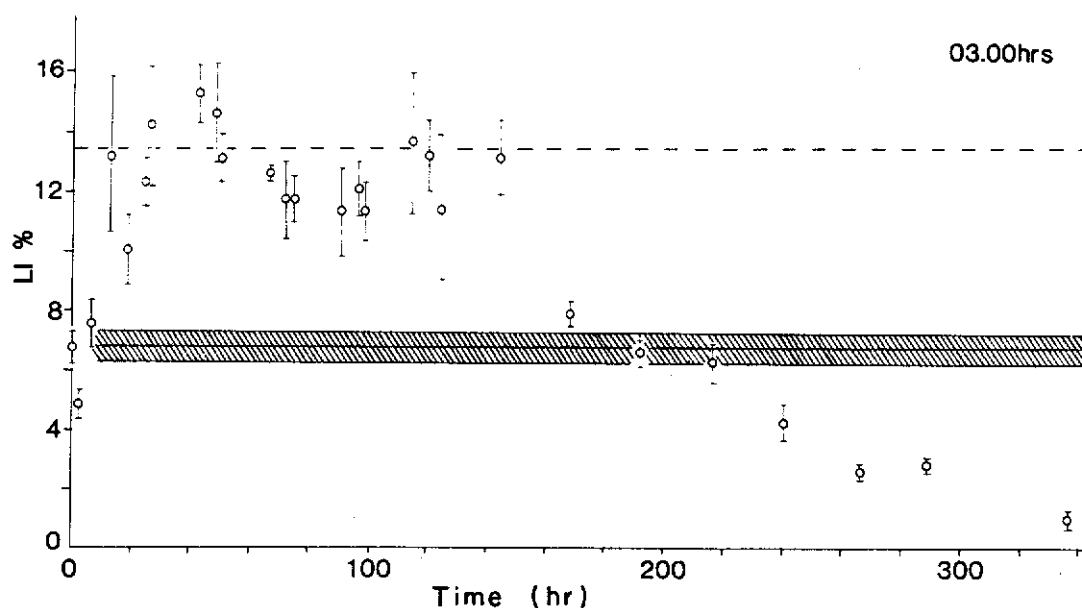

Fig. 2. The percentage of labelled cells (LI%) in autoradiographs of epidermal sheets from samples taken at various times up to 340 hr after a single injection of tritiated thymidine (25 μCi) at 03.00 hours. Each point represents the mean ± SEM for between four and sixteen mice. The shaded area represents the mean and standard error of the control point 40 min after a single injection of tritiated thymidine. The dashed line represents the LI value that is double the initial value.

Figure 3 shows the changes in LI with time after a single injection of [³H]TdR at 15.00 hours. The initial LI is 3·4%, almost exactly half that obtained at 03.00 hours. Values twice the initial LI (6·8%) are reached by about 15 hr. There is a further slight rise to about 8%. High LI values are maintained for a period, and about 18 hr after the initial doubling in LI there is a fall to levels about 1·4 times the initial LI. There is a slight increase in LI between 130 and 140 hr, which is followed by a steady fall to values of about 1% at 336 hr.

Figure 4 shows the experimental PLM results obtained when [³H]TdR is given at 03.00 hours. The G_2 period would appear to be very short (less than 2 hr). There is a narrow first peak reaching 90% about 5 hr after [³H]TdR administration. The width of this peak suggests an average T_s value of about 8 hr. There is considerable scatter of the data and a high level of 'noise', but a peak can clearly be detected at about 190 hr. However, when longer exposures or lower grain thresholds for labelled cells are used, a second earlier peak can be seen at about 80–85 hr, which has the same height as the 190-hr peak (i.e. about 20–25% labelled mitoses). Changes in exposure or threshold do not appear to influence the first or last peaks
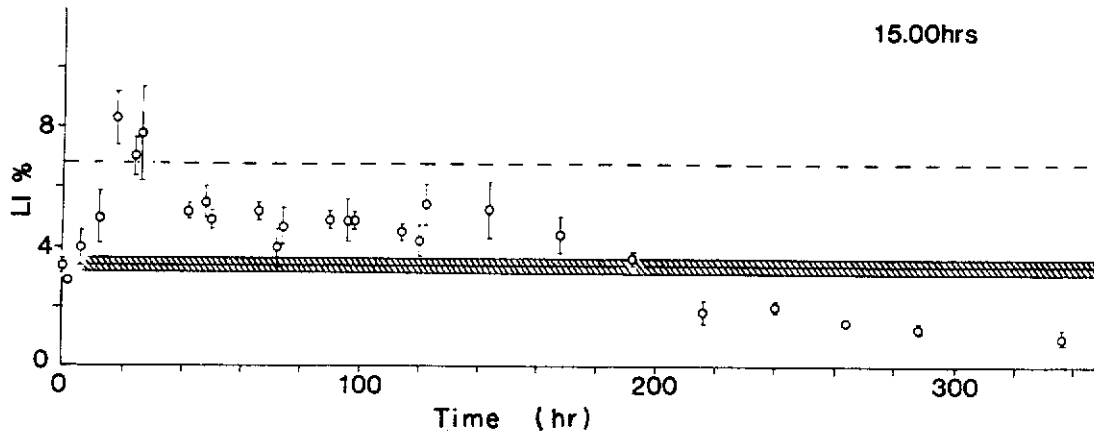
Fig. 3. Labelling index determined from autoradiographs of epidermal sheets obtained for various times up to 340 hr after a single injection of tritiated thymidine at 15.00 hrs. The experiment is otherwise identical to that shown for Fig. 2.
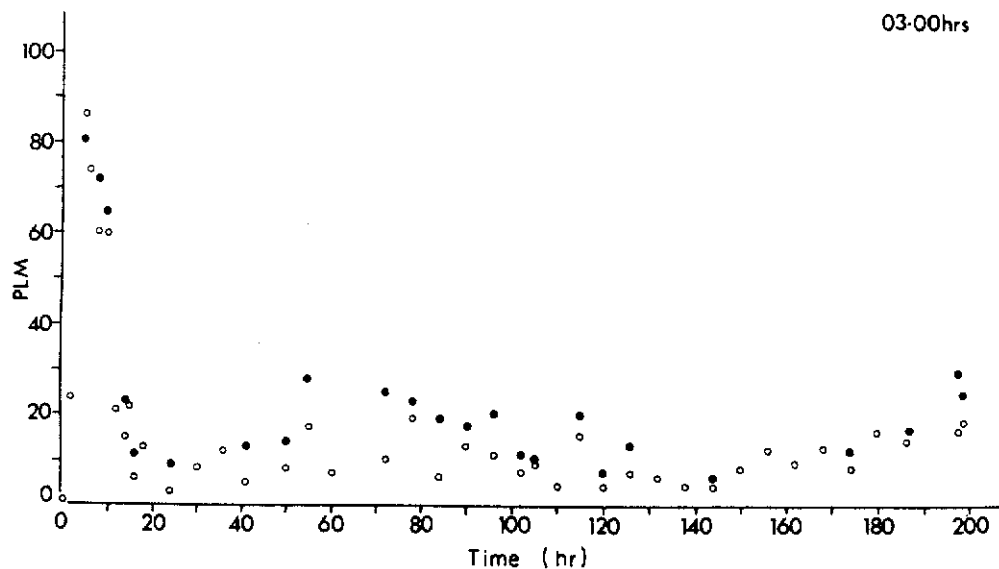

Fig. 4. Results of an experiment where 144 male 7–8 week old DBA2 mice were injected with 25 μC of [³H]TdR at 03.00 hours and groups of four mice were sampled at various times up to 200 hr thereafter. A total of 100 mitoses were analysed for each group of four mice from autoradiographs of Feulgen stained sections. The percentage of labelled mitoses (PLM) is plotted against the time after the tritiated thymidine injection. Open circles are points obtained using a 2-week exposure with a threshold of three grains per nucleus for a labelled cell. Closed circles are points obtained for longer exposure times or a lower threshold (2 grains) for labelled cells.

significantly. This suggests that the second peak is due to a discrete subpopulation of cells that are characterized by: (1) a 60–80-hr T_C and (2) a lower [³H]TdR uptake possibly because of a larger endogenous TdR pool or a long T_S (low rate of DNA synthesis).

Figure 5 shows the results of a PLM experiment where the [³H]TdR was given at 15.00 hours. The following features are apparent: (1) T_{G_2} is longer than in Fig. 3 (up to 6 hr); (2) T_S would appear to be about 7–8 hr; (3) the height of the first peak is again less than 100% and is somewhat dependent on exposure time or grain threshold; (4) a clear peak can be detected at about 190 hr; (5) a peak that is composed of cells with inherently low grain densities can again be detected at 95–100 hr; and (6) a possible small peak may be seen at about 132 hr.
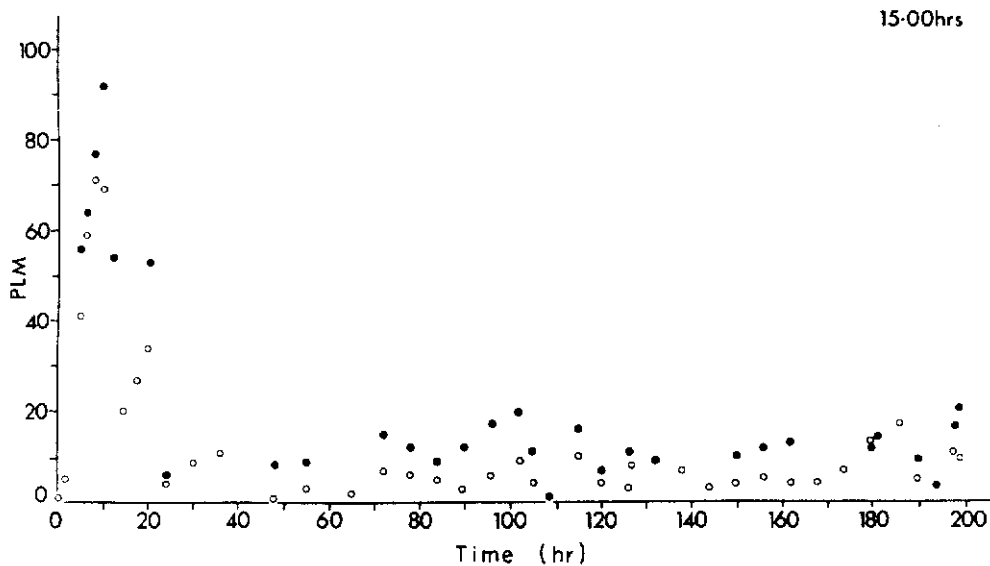
Fig. 5. Percentage labelled mitoses (PLM) curve obtained when the tritiated thymidine is injected at 15.00 hours. The experiment is otherwise identical to that illustrated in Fig. 4.

Thus, the general behaviour of cells labelled at 15.00 hours is very similar to that of cells labelled at 03.00 hours.

The following general points can be made from the PLM data: (1) the first peaks do not appear to reach 100%; (2) two subsequent peaks can be detected, both reaching about 20% labelled mitoses. However, although we recognize that these later peaks may be open to question, we believe they are real because: (a) they occur at times that are in accord with other published PLM experiments (Hegazy & Fowler, 1973; Gelfant quoted in Potten, 1980) where clearly significant peaks were reported; (b) there is a clear peak in the LI curve (03.00 hours) which can only result from a burst of labelled mitoses; and (c) a statistical significance test for time series analysis (Wallis & Moore, 1941) for the average data points between 20 and 200 hr for both the 03.00 and 15.00 hours experiments show that the hypothesis that these oscillations merely represent 'random noise' can be rejected ($P < 0.05$). Furthermore, for the 15.00 hours data, a sine wave around an average with maxima at 100 and 200 hr had a least squares error of 10.8, which is less than the least squares error of 13.2 for an average straight line. For the 03.00 hours data the corresponding values show an even greater difference (19.0 for the sine wave and 46.8 for the straight line). Thus, there is clear statistical evidence for the existence of second and third peaks in the PLM data at about 100 and 200 hr.

The results for the published continuous labelling experiments using DBA2/J mice are shown in Fig. 6. There is considerable scatter of the data points, some of the reasons for which are discussed elsewhere (Potten & Major, 1980). The curve has an initial shallow slope which is followed by a steeper rise, starting at 10 hr and continuing until it reaches 70–80% at about 100 hr. The curve may continue to rise with a slightly shallower slope thereafter but it is difficult to define the final slope with the available data.

A comparison of the various models shown in Fig. 1 and the experimental data

It is impossible to find the one most appropriate model for epidermis from amongst those shown in Fig. 1, using only the data from the three experiments described, since several of the different models may result in very similar theoretical curves. It is therefore necessary to

Fig. 6. Data obtained from experiments where tritiated thymidine (5 μCi) was injected every 3 hr into DBA2 mice and groups of mice were sampled 40 min after successive injections. Autoradiographs of sheets of epidermis were prepared and the fraction of labelled nuclei determined. The labelling index (LI%) is plotted against the time of continuous (repeated) labelling (CL). Most of the data points come from an experiment reported by Potten *et al.* (1974) recently reviewed and updated (Potten & Major, 1980).
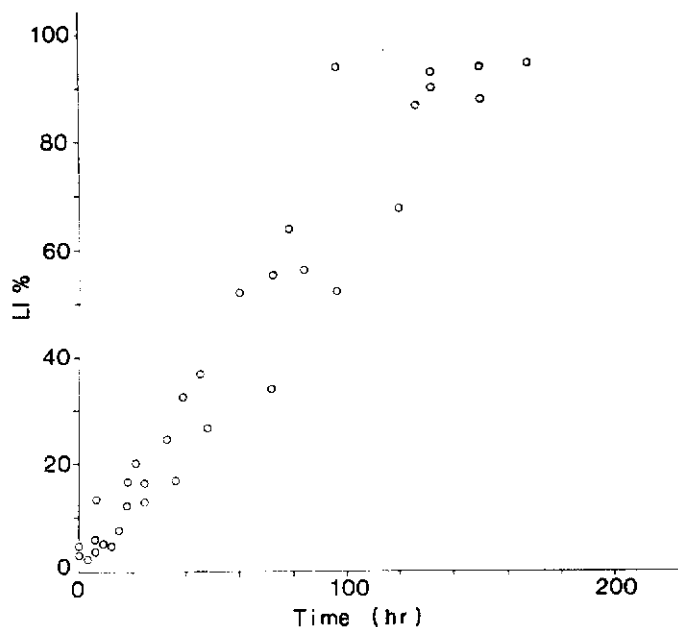
consider simultaneously the various time-independent parameters which have been defined in formulae (27)–(36) of the appendix for which some experimentally derived values are available (Table 1).

Model 1

Model 1 can be rejected on a number of grounds. (1) In the LI experiment the labelling would remain constant with time (Fig. 7) and this is not observed. (2) The clonogenic fractions would be 0·85; however, the observed values are less than 0·1. (3) The PLM curves would be expected to reach nearly 100% for the first peak when T_s is as long as 10 hr (Fig. 7). This was not always observed (Figs 4 and 5; Iversen, Bjerknes & Devik, 1968). (4) If it is assumed that the small second peak on the PLM results only from dampening due to statistical variation then a third peak would not be expected; however, a third peak of about the same size is seen (Figs 4 and 5; Potten, 1980). (5) Mitotic figures would tend to be orientated at right angles to the basement membrane and this is contrary to published observations (Smart, 1970; Duffill *et al.*, 1977). Furthermore, suprabasal labelled cells would be expected soon after labelling which is not observed (Potten, 1975b; Iversen *et al.*, 1968).

Model 2

Model 2 can be rejected also on a number of grounds. (1) In the labelling index experiment a series of repeating peaks of about the same height would be expected with the LI falling to nearly the initial value between peaks (Fig. 7); this was not observed. (2) The clonogenic fraction would be about 0·6 which is contradicted by the experimental data (Table 1). Points (3) and (4) apply as for model 1 above.

Models 3–5

If all proliferative compartments have the same cell cycle phase lengths identical labelling curves would be obtained i.e. models 3–5 would lead to the same curves as model 2. Therefore, this situation for models 3–5 can be rejected on the grounds (1), (3) and (4) above. If there were clear indications that four completely different sets of cell cycle parameters were necessary

C. S. Potten et al.

Table 1. A comparison of various cell kinetic parameters for the various models considered (time in hr)

Model type (see Fig. 1)		1[e]	2[a]	3[a]	4[a]	5[a]	5[a]	5[b]	5[c,d]	Data[d]
Corresponding labelling curves		Fig. 7	Fig. 7	Fig. 7	Fig. 7	Fig 7	Fig. 8	Fig. 9	Fig. 10	Fig. 10
Cell cycle and phase times of the compartments										
A	T_C	100	100	100	100	100	100	200	180	—
	T_s	10	10	10	10	10	4	10	2·5 (2, 3)	—
T_1	T_C	—	—	100	100	100	100	200	180	—
	T_s	—	—	10	10	10	6	10	8 (6, 10)	—
T_2	T_C	—	—	—	100	100	100	200	90	—
	T_s	—	—	—	10	10	8	10	15 (9, 21)	—
T_3	T_C	—	—	—	—	100	100	100	90	—
	T_s	—	—	—	—	10	10	5	15 (9, 21)	—
P	$T_{1/2}$	—	30	30	30	30	30	30	30	—
New cells per day	NC	0·25	0·14	0·14	0·14	0·14	0·14	0·11	0·13	0·12[f]
Proliferative fraction	PF	0·85	0·59	0·59	0·59	0·59	0·59	0·66	0·61	0·7[f]
Clonogenic fraction	CF	0·85	0·59	0·30	0·15	0·07	0·07	0·11	0·12	0·05–0·1
Average cell cycle time	T_C	100	100	100	100	100	100	167	126	120[f]
Average S-phase time	T_s	10	10	10	10	10	8·8	8·3	14·1 (8·5, 19·8)	12·5[f]
Basal layer transit time	T_{BL}	0	43	143	243	343	343	543	403	—
Initial labelling index (%)	LI_0	8·5	5·9	5·9	5·9	5·9	4·9	3·3	6·9 (4·2, 9·5)	5·3 (3·5, 7·0)
Correcting factors[g]	f	1·0	0·59	0·59	0·59	0·59	0·56	0·66	0·61 (0·63, 0·60)	—
	f_1	1·0	1·0	1·0	1·0	1·0	0·94	1·0	1·0 (1·02, 0·98)	—
	f_2	1·0	0·70	0·70	0·70	0·70	0·70	0·78	0·72	—

(a) In all compartments: $T_{G_2} = 5$ hr; $T_M = 1$ hr; $T_{G_1} = T_C - T_s - T_{G_2} - T_M$.

(b) In compartment T_3, $T_{G_2} = 2·5$ hr; $T_M = 0·5$ hr; the rest as under a.

(c) T_{G_2} and T_M see Fig. 10.

(d) The parameters in brackets represent the circadian minima and maxima. The values shown here are taken from various reports (Potten & Hendry 1973, Potten 1974, 1975a, b) or from the experiments presented here.

(e) With the constant value $LI(t) = LI$.

(f) With large experimental error.

(g) $f_3 = 0·85$ in all cases assuming 15% clear cells.

to generate theoretical curves to fit the data, then it would be possible to say that at least three transit populations exist. Since this is not possible, there is only one parameter which permits us to discriminate between these three models, i.e. between 1, 2 or 3 transit compartments, and
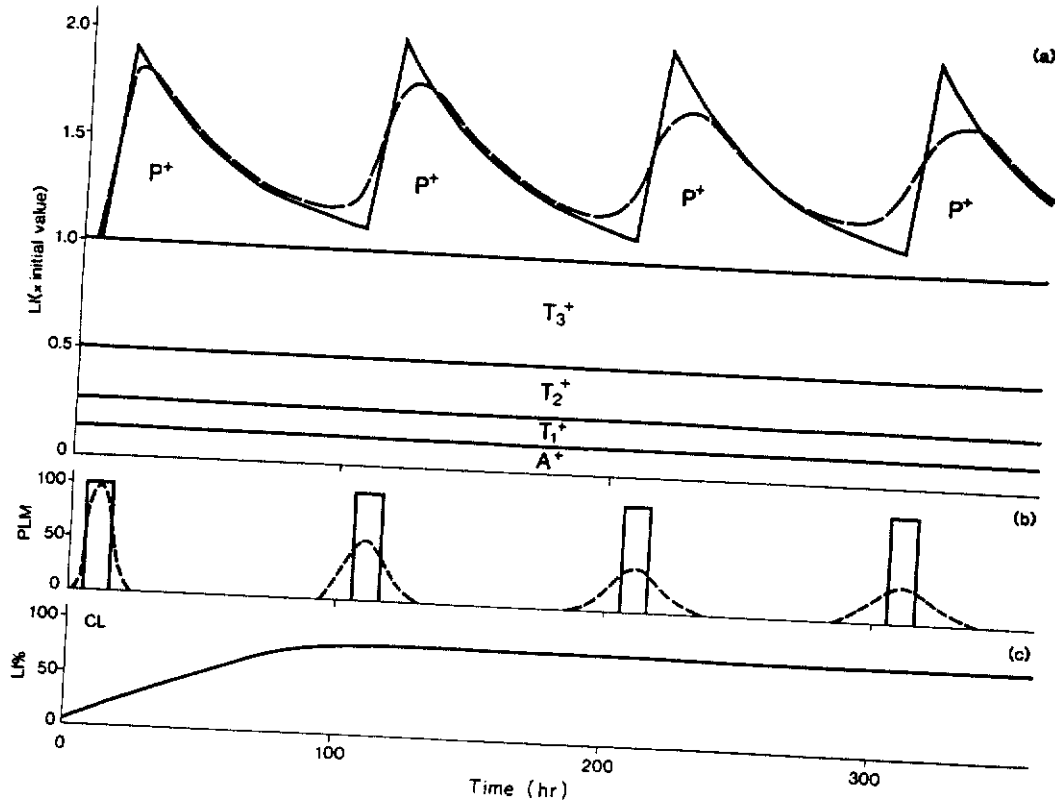
Fig. 7. Theoretical labelling curves for a homogeneous basal layer where all proliferative cells have the same cell cycle parameters: $T_C = 100$ hr, $T_s = 10$ hr, $T_{G_1} = 5$ hr, $T_M = 1$ hr; $T_{\frac{1}{2}} = 30$ hr for the post-mitotic compartment P. The theoretical curves for models 2 to 5 are identical and only model 5 will be discussed. Solid line: idealized case (no variation of the cell cycle parameters). Dashed line: realistic case (with a coefficient of variation of about 10% on the cell cycle parameters). (a) LI-curve: this shows equally spaced peaks at about 20, 120, 220 hr, etc. The peaks arise from the Labelled T_3^+ cells which enter the post-mitotic compartment as labelled cells P^+. They then leave the layer with an exponential decay. For model 1 (no post-mitotic compartment) no peaks would be seen, i.e. the results would show a straight line at $LI = 1.0$. The height of the peaks is virtually equal in the idealized case (the first peak being slightly smaller because of the decay kinetics of the P^+ cells). In the realistic case the damping effect decreases the height of the peaks slightly. How the LI curves are constructed from the labelled cells in each compartment (A^+, T_1^+, T_2^+, T_3^+ & P^+) is shown in Fig. 8 in more detail. (b) PLM-curve: this shows equally spaced peaks at 10, 110, 210, 310 hr, etc. which would occur about 10 hr earlier than the corresponding LI peaks. Here the statistical variation has a large influence on the height of the peaks. However, the area under the idealized and realistic peaks would in each case be equal. (c) CL-curves: the curve is nearly linear between 10 and 100 hr where maximum labelling (85%) is reached. Statistical variations have little influence.

this is the clonogenic fraction (CF). Clearly the evidence available at the moment on CF suggests that model 5 is the most appropriate. However, models involving more than three transit populations could also be considered. Models with T_4 or T_5 compartments would have curves similar to those in Fig. 10. These would have clonogenic fractions of 6 or 3% which correspond to 16 or 32 cells per EPU, respectively. This follows from the fact that the CF is the inverse of the cells per EPU, assuming 1 stem cell per EPU. Since the number of basal cells per EPU is 10·6 this argues against the presence of T_4 and T_5. When the experimental data shown in Figs 2–6 are compared with the theoretical curves (Figs 7–9) we find that Figs 8 and 9 are both good fits to the data for the first 200 hr, with the possible exception of the CL data, where Fig. 9 seems to be slightly better. Beyond the first 200 hr the experimental LI data do not fit either Figs 8 or 9 very well. Various features on Figs 8 and 9
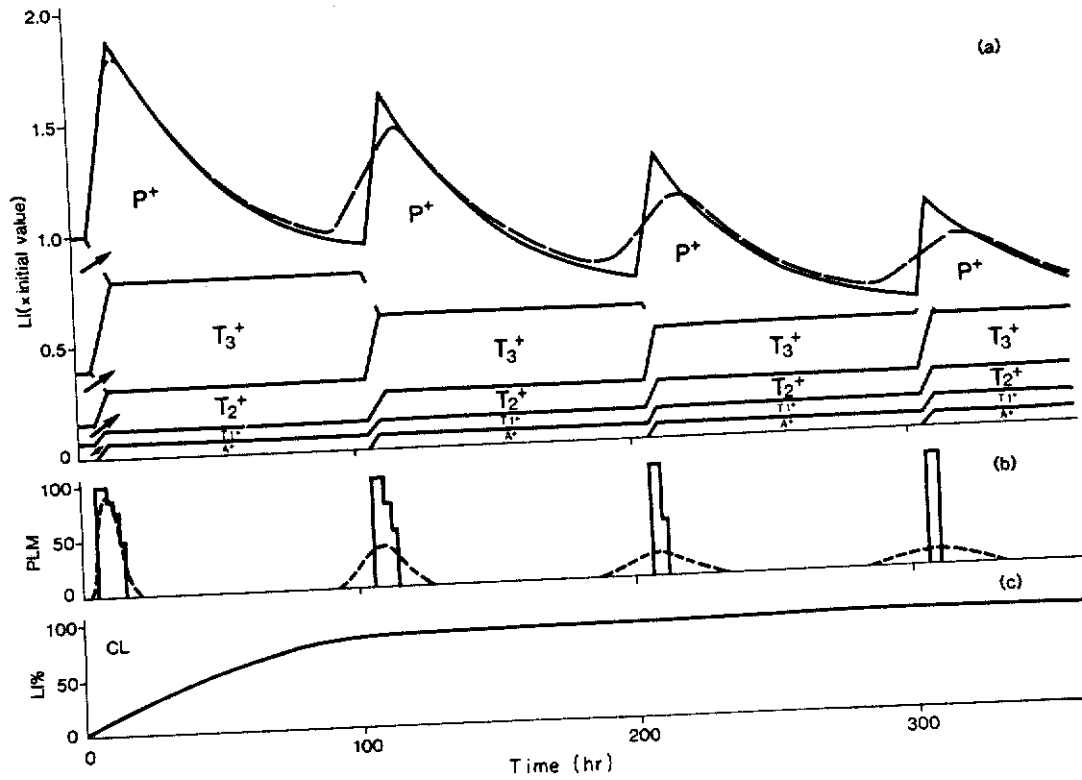
Fig. 8. Theoretical labelling curves for an inhomogeneous basal layer where subpopulations differ only in S-phase durations, i.e. T_C, T_{G_2} and T_M are equal in all compartments: $T_C = 100$, $T_{G_2} = 5$ hr, $T_M = 1$ hr, while T_S increases within the proliferative compartment. $T_S^A = 4$ hr, $T_S^{T_1} = 6$ hr, $T_S^{T_2} = 8$ hr, $T_S^{T_3} = 10$ hr. The half-life in P is $T_\frac{1}{2} = 30$ hr. The labelling curves are only shown for model 5 (solid line: idealized case; dashed line: realistic case). (a) LI-curve: this shows equally spaced peaks, since the cell cycle time in all the compartments is the same. However, the successive peak heights decrease because the S-phase times increase from A to T_3; this is easily seen by looking at the labelled cells in the various compartments. The size of each 'box' is dependent on T_S and the number of divisions each cell has undertaken. As can be seen, the second T_3^+ 'box' (labelled T_3 cells) can only be derived by a doubling of the preceding labelled T_2^+ cells and so on. The movement of labelled cells is shown by the arrows at the first mitosis. (b) PLM-curve: the peaks for the idealized case now have a step-form due to the different T_S values. From one peak to the next the most mature cells leave the proliferative compartment, and thus successive small components (steps) of the peaks are lost. Finally (after 310 hr), the peaks are determined only by the originally labelled stem cells. The width of this peak thus equals T_S^A. Statistical variation smooths and damps the peaks, one consequence being that the realistic curve for the first peaks does not reach 100%. (c) CL-curve: this is very similar to that in Fig. 7.

have been combined and elaborated in order to obtain a better overall fit to the data. This is shown in Fig. 10 along with the experimental points from Figs 2–6.

The parameters defining this 'optimum' curve are: (1) an increase in T_S from A to T_3 by a factor of 4·5 for the 03.00 and a factor of 7 for the 15.00 hours data; (2) a longer T_C in the stem cell compartment than in the later transit compartments; (3) a longer T_M in the stem cell compartment than in the transit populations.

In order to generate the progressive decline in LI for times beyond 200 hr, we need a large increase in T_S as the cells pass from the stem to the later transit populations, the last of which must have a T_C of about 100 hr. This results in a progressive reduction in peak height in the PLM. The T_C of the stem and earlier transit compartments must be nearly integer multiples of this value. If this were not so intermediate peaks would be seen in both LI and PLM curves. Although there is the slight suggestion of this in some of the PLM data (see Fig. 5), on the
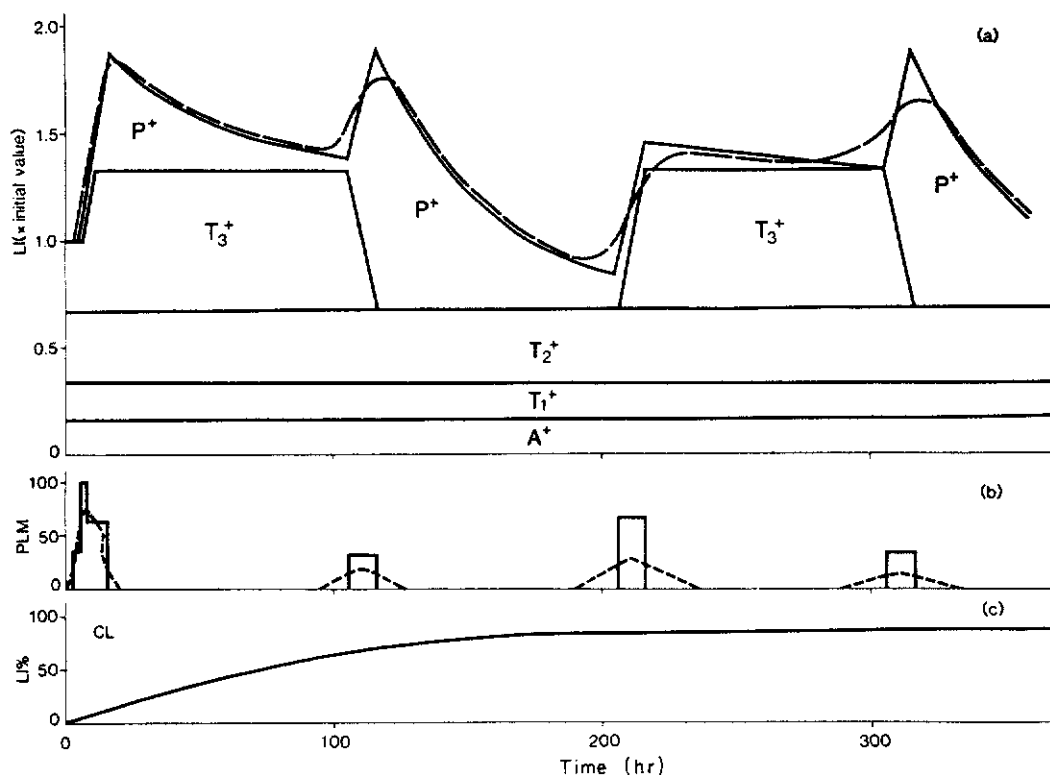
Fig. 9. Theoretical labelling curves for an inhomogeneous basal layer where the subpopulations have several differences in cell cycle parameters. For the last proliferative compartment (T_3), we chose $T_C = 100$ hr, $T_S = 5$ hr, $T_{G_2} = 2 \cdot 5$ hr, $T_M = 0 \cdot 5$ hr. All other compartments were assumed to have values double these for all phases. The half-life in P is $T_{\frac{1}{2}} = 30$ hr. The theoretical curves for models 3–5 are identical, and only those for model 5 are discussed. (Solid line: idealized case; dashed line: realistic case.) (a) LI-curve: the interval between the first two peaks corresponds to the cell cycle time in T_3; the interval between the second (100 hr) and third full peak (300 hr) equals the cell cycle time in the earlier compartment. In the idealized case the height of the first two peaks is equal. At 220 hr, no labelled cells go into the post-mitotic compartment, but their number in the proliferative compartments increases. Thus, there is no peak but an increase to a plateau. At 320 hr, labelled cells enter P once more and form a third peak. This pattern would then be repeated. In the realistic case, this complex structure at later times becomes much more difficult to determine experimentally. (b) PLM-curve: in the idealized case the first peak again has a complicated structure due to the different cell cycle phase times. However, in this case the height of the second peak is only 33%, while that of the third peak is 67%, because the absolute number of mitotic cells in the first three compartments is twice the number in the last compartment (T_3) and the labelled cells in both divide at different times. This sequence of 33% and 67% peaks then would be repeated. This, however, is largely lost due to the dampening effect caused by the statistical variation. (c) CL-curve: this now shows a biphasic form with a steeper increase up to 65%, which is reached at 100 hr when all cells in T_3 and nearly all cells in P are labelled. For complete labelling of the cells in the earlier mitotic compartments, another 100 hr are necessary i.e. 85% labelling is reached by 200 hr.

whole it is not so. The last proliferative compartment must have the shortest T_C because we see a second peak in the LI curve rather than a plateau. T_C for the A compartment (T_C^A) must be 180 hr or longer. However, if it is longer, then the CF increases, being $0 \cdot 21$ for T_C^A of 360 hr and $0 \cdot 34$ for T_C^A of 720 hr. The differences in T_M have only a small effect influencing the height of the second and third peaks on the PLM. For equal values of T_M the second peak would be raised slightly and the third reduced.

We conclude that there must be an heterogeneous basal layer with respect to T_C and T_S and the best model is one composed of stem cells and post-mitotic cells with one to three
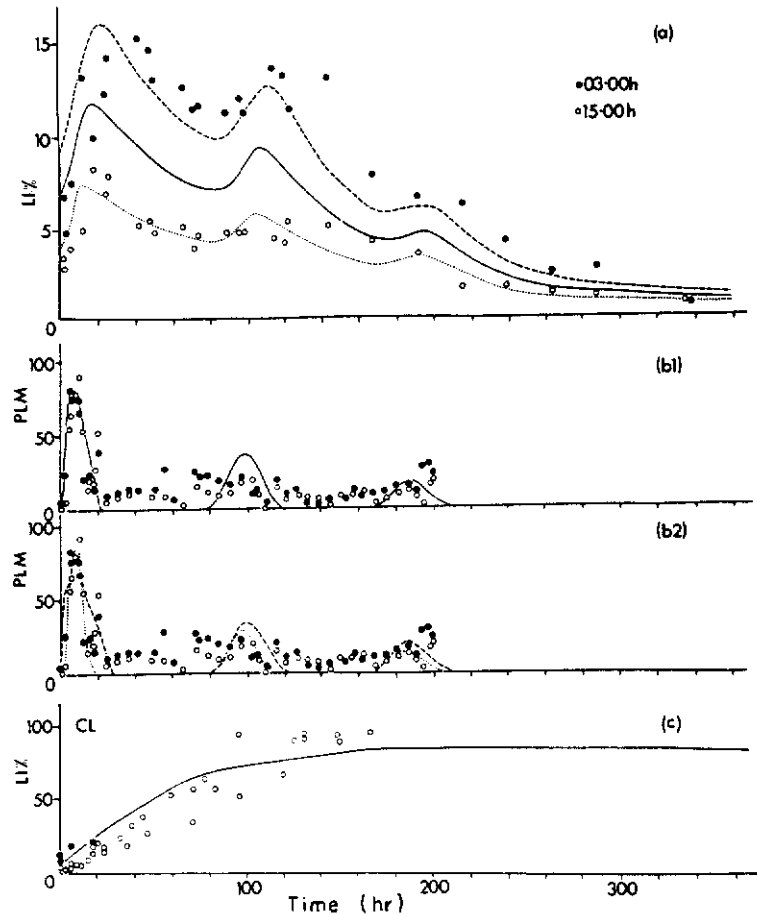
Fig. 10. A comparison of the theoretical labelling curves with the experimental data from Figs 2–6 (O, 15.00, ●, 03.00 hours). The theoretical curves are for the realistic situation (a coefficient of variation of 10%) based on the most appropriate model (see also Table 1). Since the LI depends strongly on the circadian rhythm (not fully analysed here), the minimum (dotted line), maximum (dashed line) and an intermediate situation (solid lines) have been calculated. The parameters (in hours) used for these curves are presented below for the intermediate situation (in parentheses the minimum and maximum values corresponding to the 15.00 and 03.00 hours data are shown).

	T_C	T_S		T_{G_2}		T_M	
A	180	2·5 (2, 3)		6		3	
T_1	180	8	(6, 10)	3	(4, 2)	1·5 (2, 1)	
T_2	90	15	(9, 21)	2	(3, 1)	1	(1·5, 0·5)
T_3	90	15	(9, 21)	2	(3, 1)	1	(1·5, 0·5)
Average	126	14·1 (8·5, 19·8)		2·6 (3·5, 1·8)		1·3 (1·8, 0·9)	

The half-life ($T_{\frac{1}{2}}$) in P is 30 hr.

(a) LI-curves: the theoretical curves start with an $LI_0 = 4·2$, 6·9 and 9·5%, respectively, at $t = 0$. These are, in each case, about 1·25 times the actual experimental initial values. This is necessary if the theoretical curves are to reach the first peak in experimental values. The first peaks occur at 20 hr and are about twice the initial values while the second peaks are at about 110 hr. The third peak is severely damped and occurs at 200 hr. A final LI-value of 1–2% is reached after 300 hr. The prominent decrease in the LI curves between 100 and 200 hr results from the large difference in T_S values between the earlier and the later proliferative compartments. (b1, b2) PLM curves: the theoretical curves increase to give a first maximum of about 80–85% at 10 hr. The second peaks are at 100 hr reaching 25–35%, while the third peaks at 190 hr reach 15–20%. The background 'noise' of about 5–10% is not reproduced in the theoretical curves. The width of the peaks is determined mainly by the T_S values, the half-width corresponding approximately to the average T_S. The height of the second and third peak depends on
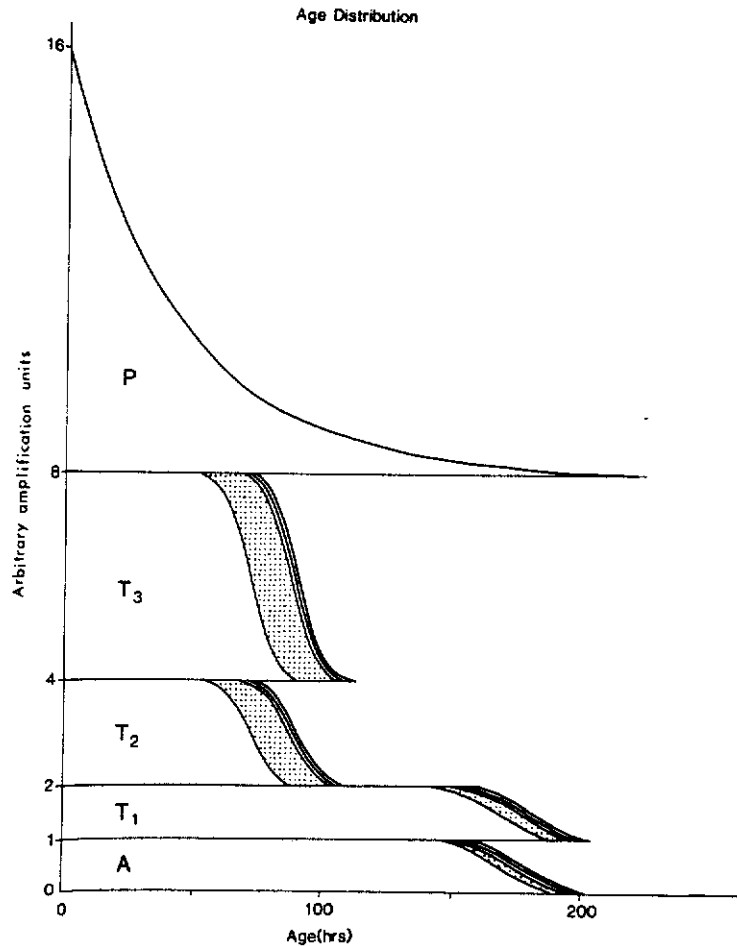
Age Distribution

Fig. 11. The age structure for the basal layer for the final model (the intermediate situation in Fig. 10). Age is measured from the birth of a cell in a compartment as shown below. A stem cell enters the S phase 145–190 hr after its last mitosis. It stops DNA-synthesis about 2·5 hr later and begins mitosis 6 hr later. Thus, a cell leaves the stem cell compartment 160–200 hr (average 180 hr) after its last mitosis. This new cell enters T_1 with age 0 and shows a behaviour pattern similar to that in A. However, T_S has increased slightly while T_M and T_{G_2} have decreased by about the same amount. After division, two cells enter T_2 where DNA synthesis begins after about 70 hr and stops 15 hr later. After a cell cycle time of 90 hr two cells leave T_2 and four cells enter T_3 with age 0 having the same cell cycle parameters as in T_2. Finally eight cells enter the post-mitotic compartment P. They leave this compartment, and thus leave the layer at random with a half-life time $(T_{\frac{1}{2}})$ in P of 30 hr. A cell born from the stem cell compartment remains in the basal layer for an average of 403 hr (16·8 days), equivalent to the basal layer transit time. The characteristics of the changes in the cell cycle parameters from A to T_3 are: T_C decreasing, T_S increasing, T_{G_2} and T_M decreasing. The ordinate is scaled in arbitrary units of amplification. The number of cells in each compartment is proportional to the area under each curve.

three factors: (1) the two different cell cycle times; (2) the different S-phase times; (3) the inverse relationship of T_M and T_S. T_{G_2} has only a minor influence on determining the position of the maximum of the first peak. (b1) is the intermediate curve while (b2) shows the minimum and maximum situations as described for the LI curves. (c) CL curves: the theoretical curve reaches 70% LI at 90 hr and then continues to rise more gradually to a maximum of 85% after 180 hr. The CL curves are not strongly affected by changes in the assumed parameters for the various models. In all three types of the experiment the theoretical curves have the same general shape and reach absolute values very similar to those obtained in experiments.

(most likely three) transit proliferative populations. The data can best be explained if there are at least two types of proliferating cells with different T_S values with the stem cell T_S being the shortest and the T_S of the terminal transit population being the longest.

Figure 11 illustrates the age distribution of this model for epidermis which was outlined in Fig. 10, age being measured as the time from the birth of a cell in a new proliferative compartment. As can be seen the overall age structure of the basal layer is complex.

DISCUSSION

LI experiments

There is one published example of an LI experiment for mouse epidermis similar in design to that reported here (Hegazy & Fowler, 1973). The results from this earlier experiment differed in several ways: (a) the timing of the first peak (10 hr instead of the 20–40 hr in Figs 2 and 3); (b) the sharpness in the rise to double the initial LI in the earlier report; and (c) the timing of the fall in LI after the first peak which is much more rapid in the earlier report. The reasons for these differences remain obscure, but may be a reflection of differences between mouse strains (the initial LI was much higher in the Hegazy & Fowler experiment) and experimental technique (sections versus sheets of epidermis).

Our experiments show the following features: (1) a strong dependence on the time of day label is administered; (2) an initial drop in LI; (3) an increase to values slightly in excess of twice the initial LI; (4) peaks at 20–40 and 110–130 hr; (5) a fairly steady decrease to values of about 1% at 336 hr without any clear sign of a third peak (even when 6-week exposures were compared with 4-week exposures).

We have not taken into account the full implication of the circadian rhythms since this is the basis of further studies. However, theoretical curves have beeen calculated using different S-phase durations which result in initial LI values similar to those observed. We do not have any clear explanation as yet for points (2) and (3) listed above. As can be seen from Fig. 10 the theoretical curves provide explanations for the timing and magnitude of the peaks and for the overall decay in LI. A good overall fit and, in particular, a fit for the final LI, can only be achieved by assuming that T_S varies as well as T_C and that T_S has a minimum value in the A compartment. The value assumed for T_S^A was 2·5 hr. However, this cannot be measured directly since the techniques available provide average values for T_S. The average T_S used in our calculations is well within the range of published values for mouse epidermis (Table 1).

PLM experiments

There are two examples in the literature where PLM experiments have been conducted on epidermis from the back of a mouse which achieve a second peak (Hegazy & Fowler 1973; Gelfant quoted in Potten, 1980). These show: (a) a first peak that reaches close to 100% within 10–20 hr, although other cases where only the first peak was presented do not reach 100% (Devik, 1962; Iversen *et al.*, 1968; Olsson, 1976); (b) minimum values within the next 10–40 hr which show remarkably little 'noise'; and (c) a second peak at 110–190 hr that reaches 30–50% labelled mitoses and has an area of about 80 or 60% of the first peak.

Our results (Figs 4 and 5) show: (1) an initial peak that reaches 90% labelled mitoses; (2) an inter-peak level of 'noise' corresponding to about 5–10%; (3) second and third peaks at 90–100 hr and about 190 hr, both reaching about 20% labelled mitoses; and (4) a second peak that is largely dependent on grain count threshold or exposure time while, the first and third are not.

There is a clear agreement between the timing of the first and second peaks when the

published curves are compared to the present data. However, there are two points of difference, namely the higher 'noise' observed in the present experiments and the fact that the first peak does not appear to reach 100%. There are also two novel features, namely the presence of a third peak and the dependence of the second peak on grain count threshold. As can be seen from Fig. 10 the theoretical curves provide an explanation for the fact that the first peak may not reach 100% and for the presence of second and third peaks of about the same size.

The fact that the first peak in the model does not reach 100% is a consequence of the heterogeneity, mainly in T_S. The model predicts that the second peak would have an area 70% that of the first. This is a consequence of the fact that, of the initially labelled cells, those that were T_3 will have left the layer, those that were T_1 and T_2 will divide after 90 hr and form the second peak, while those that were A will not divide until 180 hr (see flow chart in Fig. 8). The third peak would have an area 40% that of the first peak. The third peak is attributable exclusively to cells originally labelled as A or T_1 and these are characterized by short values for T_S, i.e. a smaller proportion labelled.

In the model the second peak is derived from cells originally labelled as T_1 and T_2 cells in the ratio 1:4, and since T_2 cells have a long T_S (and hence a slow rate of synthesis) this may be the explanation for the grain count threshold dependence. We do not have an explanation for the higher noise level. The model would predict only small 4th and 5th peaks which possibly are difficult to detect because of the high noise level. However, it is possible that in tissues with a different proliferative organization further high peaks might occur (e.g. Gelfant's data for ear epidermis quoted in Potten, 1980; Hamilton & Blackwood's results for oral mucosa, 1974). The width and area of the theoretical first peak for the 03.00 hours situation is too large. We believe this is a consequence of the simple assumptions we make concerning the circadian rhythm.

CL experiments

The CL experiments have been presented and discussed elsewhere (Potten & Major, 1980). All the data points appear to scatter about a common line but the degree of scatter is such that precise statements about levels of labelling and times of changes in slope cannot be made. We have assumed that the 15% clear cells are non-replacing and thus the theoretical CL curves plateau at 85%. In fact both Langerhans cells and melanocytes may be gradually replaced. The labelling studies of Langerhans cells suggest that their turnover is very slow (Schellander & Wolff, 1967; Wolff, 1972; Mackenzie, 1975).

The theoretical curve for the CL experiments (Fig. 10) is based on an average LI of 6·9%). The actual experiment was begun at 12.00 hours, i.e. very close to the circadian minimum. In fact the initial LI was lower than usual in this experiment at about 3·0%. If the lower initial value for 15.00 hours is used then the theoretical CL curve is slightly lower than the average curve shown in Fig. 10c. However, a slight discrepancy still remains.

Age distribution

Many published reports make the simplest assumptions about the age distribution namely that it is rectangular or a simple exponential.

As can be seen from Fig. 11 the overall age distribution for model 5 (Fig. 1; the most appropriate for epidermis) is complex, being composed of several roughly rectangular distributions and an exponential component.

A different age distribution could apply for the P compartment. This could be studied by subdividing the P compartment as was done for the A and T compartments. The consequence

would be a reduction in the coefficient of variation of the transit time for P resulting in a different age distribution lying somewhere between that shown in Fig. 11 for A, T and P. This type of approach would require additional parameters and is not a critical point for the overall conclusion. We have neglected it.

There are situations where it would be useful to estimate T_C from the LI and T_S (see equation 37, appendix). This can only correctly be done if account is taken of the overall proliferative organization in the basal layer. This involves: (1) the heterogeneity in T_S and T_C which leads to a factor f_1; (2) the exponential loss of cells assumed for the P compartment (which cannot be distinguished from a loss in G_1), factor f_2; and (3) the fact that the basal layer contains some clear cells, factor f_3. These factors are presented in the appendix and lead to an overall factor f that in the case considered (Fig. 11) has a value of 0·61. Statistical variation in cell cycle phase lengths has little influence on the value of f since this variation does not affect the areas of the age distribution. The value for f of 0·61 is only valid for situations where average daily values of T_S and LI are used, since circadian rhythms are not considered. We have assumed throughout that all mitoses are in a plane parallel to the basement membrane. There are no data on this for mouse dorsum. Loss directly to the suprabasal layers at mitosis may occur from the later transit populations. However, the fact that the LI doubles and persists at a high level for some time suggests that this is not a large complication. If, however, loss of this sort occurred from the stem cell population it would have an effect of reducing the LI in the later stages of the LI experiment. However, for this to be significant, a large fraction of stem cells would have to divide in this way, which does not seem likely from a biological point of view. In some other situations with different proliferative organization more mitoses may be at right angles (Smart, 1970), or there may be loss from other compartments (Hume, 1980) in which case an additional component is necessary for f.

Proliferative fraction

The concept of a growth or proliferative fraction as originally conceived for tumours (Mendelsohn, 1962), may at first sight appear to have little relevance for epidermis. However, there are several distinct cell types in epidermis (e.g. clear cells) and, within the keratinocyte population, subpopulations of proliferating and non-proliferating cells may exist. The overall fraction of basal cells that are actively cycling (the proliferative fraction which can be calculated by $PF = f_2 \cdot f_3$) is 0·61 (see Table 1 and equation 41, appendix).

The degrees of freedom in the model

The model has been constructed step by step. Taking into account the various different parameters used for the 03.00 and 15.00 hours experiments there are 18 degrees of freedom for the cell cycle times of the proliferative compartments. There are three additional factors that provide a further 3 degrees of freedom (the variance described by a common λ, T_1 for the P compartment, and 15% clear cells). These twenty-one independent parameters have been derived by comparison between the theoretical curves with the 7 experimental parameters in Table 1 and the five experiments in Figs 2–6 which together represent more than 160 data points.

The number of transit compartments and the exponential decrease in P used here (Fig. 10) represent a simple, but not necessarily the only, situation which can encompass all the data without major contradictions.

Further considerations

There are several additional factors which might have some influence on the use of the model and its interpretation which we have not discussed.

(1) Factors concerned with the use of thymidine or tritiated thymidine. These include: (a) possible changes induced by the use of exogeneously administered thymidine (Greulich, Cameron & Thrasher, 1961); (b) damage and changes induced by the internal irradiation from tritium (Olsson, 1977; Möller, Larsen & Faber, 1974; Post & Hoffman, 1968; Cheng & Leblond, 1974); (c) The influence in some experiments of the reutilization of tritiated thymidine from dying differentiated cells (Myers & Feinendegen, 1976; Cutright & Bauer, 1967; Hume, 1980); (d) the influence in some experiments of a delayed uptake of tritiated thymidine from long-lived intracellular pool (Moffat & Pelc, 1966; Potten, 1971, 1973; Lord, 1978; Hume & Potten, 1980).

(2) The influence, in some experiments, of the possible selective sorting of the older and newer strands of DNA in epithelial stem cells (Cairns, 1975; Potten *et al.*, 1978).

(3) The influence of the circadian rhythm on the experiments and the interpretation of the model. As already stated we have not taken these into account fully, since this is currently being investigated. Circadian rhythms are well documented (Tvermyr, 1969, 1972; Clausen *et al.*, 1979), and are clearly important (see the 2-fold difference in initial LI in Figs 2 and 3). We have assumed changes in the duration of S, but changes in the number of cells entering and leaving S may be an alternative.

Applications

Uniquely this program can be applied to situations where there is a heterogeneity in the proliferative compartment. Information on the relative importance of T_s in the stem and final transit compartment (A and T_3 in our case) can easily be obtained from the ratio of the final LI to the initial LI.

At a simple level (i.e. the idealized case) it is easy to calculate the LI, PLM and CL curves for other examples of tissues with different proliferative organization. This can be achieved without a computer using the technique described above. Furthermore our mathematical approach can easily be generalized, in which case the effect of the daily rhythm in MI or LI can be determined (this is the basis of current work). Finally, the program and model can be adopted to consider cases where the steady state is disrupted.

ACKNOWLEDGMENTS

REFERENCES

ALLEN, T.D. & POTTEN, C.S. (1974) Fine structural identification and organisation of the epidermal proliferative unit. *J. cell Sci.* **15**, 291.

CAIRNS, J. (1975) Mutation, selection and the natural history of cancer. *Nature* **255**, 197.

322   *C. S. Potten et al.*

CHENG, H. & LEBLOND, C.P. (1974) Origin, differentiation and renewal of four main epithelial cell types in the mouse intestine. V. *Am. J. Anat.* **141**, 537.

CLAUSEN, O.P.F., THORUD, E., BJERKNES, R. & ELGJO, K. (1979) Circadian rhythms in mouse epidermal basal cell proliferation. *Cell Tissue Kinet.* **12**, 319.

CUTRIGHT, D.E. & BAUER, H. (1967) Cell renewal in the oral mucosa and skin of the rat. II. *Oral Surg. Oral Med. Oral Path.* **23**, 260.

DEVIK, F. (1962) Studies on the duration of DNA synthesis and mitosis in irradiated and regenerating epidermis cells in mice, by means of tritium-labelled thymidine. *Int. J. Rad. Biol.* **5**, 59.

DUFFIL, M.B., APPLETON, D.R., DYSON, P., SHUSTER, S. & WRIGHT, N.A. (1977) The measurement of the cell cycle time in squamous epithelium using the metaphase arrest technique with vincristine. *Br. J. Derm.* **96**, 493.

GILBERT, C.W. & LAJTHA, L.G. (1965) The importance of cell population kinetics in determining response to irradiation of normal and malignant tissue. In: *Cellular and Radiation Biology*, p. 474. Williams and Wilkins Co., Baltimore.

GREULICH, R.C., CAMERON, I.L. & THRASHER (1961) Stimulation of mitosis in adult mice by administration of thymidine. *Proc. Nat. Acad. Sci.* **47**, 743.

HAMILTON, A.I. & BLACKWOOD, H.J.J. (1974) Cell renewal of oral mucosal epithelium of the rat. *J. Anat.* **117**, 313.

HEGAZY, M.A.H. & FOWLER, J.F. (1973) Cell population kinetics of plucked and unplucked mouse skin. I. Unirradiated skin. *Cell Tissue Kinet.* **6**, 17.

HUME, W.J. (1980) Proliferative organization in mouse tongue epithelium. PhD Thesis, University of Manchester.

HUME, W.J. & POTTEN, C.S. (1980) Stem cells have a long-lived TdR pool *Cell Tissue Kinet.* **13**, 199, (abstract).

IVERSEN, O.H., BJERKNES, R. & DEVIK, F. (1968) Kinetics of cell renewal, Cell migration and cell loss in the hairless mouse dorsal epidermis. *Cell Tissue Kinet.* **1**, 351.

LORD, B.I. (1978) Cellular and architectural factors influencing the proliferation of hematopoietic stem cells. In: *Differentiation of normal and neoplastic haematopoietic cells* (Ed. by B. Clarkson, P. A. Marks & J. E. Till), pp. 775. Cold Spring Harbor.

MACKENZIE, I.C. (1975) Labelling of murine epidermal Langerhans cells with ^{3}H-thymidine *Am. J. Anat.* **144**, 127.

MENDELSOHN, M.L. (1962) Autoradiographic analysis of cell proliferation in spontaneous breast cancer of C3H mouse. III. The Growth fraction. *J. nat. Cancer Inst.* **28**, 1015.

MOFFAT, G.H. & PELC, S.R. (1966) Delay after plucking of hairs between the appearance of ^{3}H-thymidine in cells and its incorporation into DNA. *Exp. Cell Res.* **42**, 460.

MÖLLER, U. LARSEN, J.K. & FABER, M. (1974) The influence of injected tritiated thymidine on the mitotic circadian rhythm in the epithelium of the hamster cheek pouch. *Cell Tissue Kinet.* **7**, 231.

MYERS, D.K. & FEINENDEGEN, L.E. (1976) DNA tumour and thymidine reutilisation in mouse tissues. *Cell Tissue Kinet.* **9**, 215.

OLSSON, L. (1976) Effects of tritium-labelled pyrimidine nucleosides on epithelial cell proliferation in the mouse. *Rad. Res.* **68**, 258.

POST, J. & HOFFMAN, J. (1968) Early and late effects of ^{3}HTdR labelled DNA on Ileal cell replication *in vivo*. *Rad. Res.* **34**, 570.

POTTEN, C.S. (1971) Early and late incorporation of tritiated thymidine into skin cells and the presence of a long-lived G_0-specific precursor pool. *J. Cell Biol.* **51**, 855.

POTTEN, C.S. (1973) Further observations on the late labelling associated with stimulus-responsive cells in skin. *Cell Tissue Kinet.* **6**, 533.

POTTEN, C.S. (1974) The epidermal proliferation unit: the possible role of the central basal cell. *Cell Tissue Kinet.* **7**, 77.

POTTEN, C.S. (1975a) Epidermal cell production rates. *J. Invest. Derm.* **65**, 488.

POTTEN, C.S. (1975b) Epidermal transit times. *Br. J. Derm.* **93**, 649.

POTTEN, C.S. (1980) Cell replacement in epidermis (keratopoiesis) via discrete units of proliferation. *Int. Rev. Cytol.* **69**, 271.

POTTEN, C.S. & HENDRY, J.H. (1973) Clonogenic cells and stem cells in epidermis. *Int. J. Rad. Biol.* **24**, 537.

POTTEN, C.S., HUME, W.J., REID, P. & CAIRNS, J. (1978) The segregation of DNA in epithelial stem cells. *Cell*, **15**, 899.

POTTEN, C.S., KOVACS, L. & HAMILTON, E. (1974) Continuous labelling studies on mouse skin and intestine. *Cell Tissue Kinet.* **7**, 271.

POTTEN, C.S. & MAJOR, D. (1980) Repeated injection (continuous labelling) experiments in mouse epidermis. *J. Theoret. Biol.* **82**, 465.

SCHELLANDER, F. & WOLFF, K. (1967) Zur Autoradiographischen Markierung von Langerhandzellen mit ³H-thymidin. *Arch. Klin. exp. Derm.* **230**, 140.

SMART, I.H.M. (1970) Variation in the plane of cell cleavage during the process of stratification in the mouse epidermis. *Br. J. Derm.* **82**, 276.

TVERMYR, E.M.F. (1969) Circadian rhythms in epidermal mitotic activity. *Virchows Arch. Abt. B. Zellpath.* **2**, 318.

TVERMYR, E.M.F. (1972) Circadian rhythms in hairless mouse epidermal DNA synthesis as measured by double labelling with ³H-thymidine (HTdR) *Virchows Arch. Abt. B. Zellpath.* **11**, 43.

WOLFF, K. (1972) The Langerhans cell. *Current problems Derm.* **4**, 79.

WALLIS, W.A. & MOORE, G.H. (1941) A significance test for time series analysis. *J. Am. Statist. Ass.* **36**, 401.

APPENDIX

As illustrated in Fig. 1 the basal layer of the epidermis may be composed of as many as five different cellular compartments, designated A, T_1, T_2, T_3 and P. Mathematically, each of these compartments can be regarded as being subdivided into n subcompartments. By assuming a random substructure we can arrive at the number of cells y_i in any subcompartment i through the differential equation:

$$\dot{y}_i(t) = z_i(t) - \lambda_i y_i(t) \qquad i = 1, \ldots, n \tag{1}$$

with the initial value $y_i(0)$, and hence the total compartment size is:

$$Y_C(t) = \sum_{i=1}^{n} y_i(t) \tag{2}$$

where $Y_C(t)$ is an abbreviation for the number of cells in the compartments shown in Fig. 1:

$$Y_C(t) = A(t), T_1(t), T_2(t), T_3(t), P(t). \tag{3}$$

The influx rate $z_i(t)$ into each subcompartment $i (i = 1, \ldots, n)$ depends on the nature of the compartment. For example, for the stem cells $[Y_C(t) = A(t)]$ we have:

$$z_i(t) = \begin{cases} \lambda_n y_n(t) & i = 1 \\ \\ \lambda_{i-1} y_{i-1}(t) & i = 2, \ldots, n \end{cases} \tag{4}$$

i.e. after mitosis in the stem cell compartment half the new cells stay as stem cells while the remainder move into the first of the transit compartments where $Y_C(t) = T_1(t)$. Here we have:

$$z_i(t) = \begin{cases} \lambda_n^* y_n^*(t) & i = 1 \\ \\ \lambda_{i-1} y_{i-1}(t) & i = 2, \ldots, n \end{cases} \tag{5}$$

where $\lambda_n^* y_n^*(t)$ is the influx rate coming from the last subcompartment of A.

However, in the further transit compartments and in the post-mitotic compartment $[Y_C(t) = T_2(t), T_3(t), P(t)]$ we have:

$$z_i(t) = \begin{cases} 2\lambda_n^* y_n^*(t) & i = 1 \\ \\ \lambda_{i-1} y_{i-1}(t) & i = 2, \ldots, n \end{cases} \tag{6}$$

$\lambda_n^* y_n^*(t)$ is again the efflux rate from the last subcompartment of the preceding compartment. In every subcompartment i, the transit time is exponentially distributed with the average transit time $1/\lambda_i$ with a variance of $1/\lambda_i^2$.

For all the proliferative compartments we have considered the cell cycle phases as separate groups of subcompartments, e.g. n_{G_1} corresponds to the number of subcompartments in G_1; n_S represents the number in S phase etc. If Y_x is the number of cells where $x = G_1$, S, G_2, M, C denotes the various phases of the cycle or the total cell cycle respectively we find:

$$Y_x(t) = \sum_{i=l_x}^{m_x} y_i(t) \text{ (cell number)} \tag{7}$$

$$T_x = \sum_{i=l_x}^{m_x} \frac{T}{\lambda_i} \text{ (average transit time)} \tag{8}$$

$$\sigma_x^2 = \sum_{i=l_x}^{m_x} \frac{1}{\lambda_i^2} \quad \text{(variance of the average transit time)} \tag{9}$$

$$\sigma_x/T_x \quad \text{(coefficient of variation)} \tag{10}$$

with

$l_x = 1, \quad m_x = n_{G_1} \text{ for } x = G_1 \text{ (G}_1\text{-phase)}$

$l_x = n_{G_1} + 1, \quad m_x = n_{G_1} + n_s \text{ for } x = S \text{ (S-phase)}$

$l_x = n_{G_1} + n_s + 1, \quad m_x = n_{G_1} + n_s + n_{G_2} \text{ for } x = G_2 \text{ (G}_2\text{-phase)}$

$l_x = n_{G_1} + n_s + n_{G_2} + 1, \quad m_x = n \text{ for } x = M \text{ (M-phase)}$

$l_x = 1, \quad m_x = n \text{ for } x = C \text{ (total cell cycle)}$

$$n = n_{G_1} + n_s + n_{G_2} + n_M \tag{11}$$

The parameters λ and $n_{G_1}, n_s \ldots$ should be determined from the experimental data, but since there are too many variables (giving too many degrees of freedom) it is convenient to assume that some or all of the λ_i are equal. If we assume all λ_i to be equal

$$\lambda = \lambda_i \qquad i = 1, \ldots, n \tag{12}$$

then formulae (8), (9), (10) simplify to:

$$T_x = \frac{n_x}{\lambda}, \qquad \sigma_x^2 = \frac{n_x}{\lambda^2}, \qquad \sigma_x/T_x = \frac{1}{\sqrt{n_x}} \tag{13}$$

with $x = G_1, S, G_2, M, C$.

The corresponding transit times through the phases or cycle are gamma distributed with

$$f(a) = \frac{\lambda^{n_x} a^{n_x - 1}}{(n_x - 1)!} e^{-\lambda a} \tag{14}$$

where n_x represents $n_{G_1}, n_s, n_{G_2}, n_M, n$.

For the post-mitotic compartment P we have assumed a random loss from the basal layer to the layer above requiring only one parameter, λ_p. This gives an exponential age distribution:

$$f(a) = \lambda_p e^{-\lambda_p a} \tag{15}$$

with a half-life of

$$T_{\frac{1}{2}} = T_p . \ln 2 \quad \text{with} \quad T_p = 1/\lambda_p \tag{16}$$

where T_p is the average transit time through P.

Labelled cells

The same considerations can also be used to describe the subpopulation of tritiated thymidine labelled cells which will be noted by the superscript [†].

All cells in the S-phase in populations A, T_1, T_2 or T_3 are assumed to be labelled at time 0; all other cells being unlabelled

$$\dot{y}_i^\dagger(t) = z_i^\dagger(t) - \lambda_i y_i^\dagger(t) \qquad i = 1, \ldots, n \tag{17}$$

with the initial value

$$y_i^\dagger(0) = \begin{cases} y_i(0) & i = n_{G_1} + 1, \ldots, n_{G_1} + n_s \\ \\ 0 \text{ else} \end{cases}$$

and hence the number of labelled cells is

$$Y_C^\dagger(t) = \sum_{i=1}^{n} y_i^\dagger(t) \quad \text{(number of labelled cells in the total compartment)} \tag{18}$$

$$Y_M^\dagger(t) = \sum_{i=n-n_M+1}^{n} y_i^\dagger(t) \quad \text{(number of labelled cells in the M phase)}$$

where $z_i^\dagger(t)$ is defined as was $z_i(t)$ in (4), (5), (6) with $y_{i-1}^\dagger$ instead of y_{i-1}.

Steady state

For the special case where the system is in a steady state, the cell numbers in subcompartment i and phase x are denoted by y_i and Y_x respectively. Then:

$$y_i = 0, \qquad \lambda_i y_i = \text{const} = :z, \qquad i = 1, \ldots, n \tag{19}$$

and for the numbers of cells in the compartments

$$Y_x = \sum_{i=l_x}^{m_x} y_i = z \sum_{i=l_x}^{m_x} \frac{1}{\lambda_i} = z . T_x \tag{20}$$

with $x = G_1, S, G_2, M, C$ and l_x, m_x in (11). When $x = C$, Y_C denotes the constant number of cells in steady state in each of the compartments of Fig. 1

$$Y_C = A, T_1, T_2, T_3, P \tag{21}$$

which is analogous to (3). T_C represents the corresponding cell cycle times (which are, of course, not necessarily equal), while the parameter z is the steady state influx rate or cell production rate. For steady state conditions the number of cells Y_C in a compartment can be calculated from the product of the influx z and the cell cycle time T_C ($Y_C = z . T_C$). This product represents the area under each curve in Fig. 11.

Simplification for the case without variation

If we consider the simple case of a 'first in, first out' structure in compartments A, T_1, T_2, T_3 and P without any variation in the phase times and cell cycle times, then, in the formula used above, the number n of subcompartments must increase to infinity (in which case the limit of equation (14) becomes a rectangular age distribution). We can deal with this situation more easily with the discrete formulation below: compartment $Y_C(t)$ is divided into n subcompartments $y_i(t)$, $i = 1, \ldots, n$ which represent cell cycle age classes of length Δt of equal size. Then we find

$$y_i(t + \Delta t) = y_{i-1}(t) \qquad i = 2, \ldots, n \tag{22}$$

$$y_1(t + \Delta t) = \begin{cases} y_n(t) & \text{for compartment A} \\ y_n^\dagger(t) & \text{for compartment } T_1 \\ 2 y_n^\dagger(t) & \text{for compartments } T_2, T_3, P \end{cases} \tag{23}$$

where $y_n^\dagger(t)$ is the number of cells in the last subcompartment of the preceding compartment. Here we have

$$T_C = n . \Delta t, \qquad \sigma^2 = 0 \tag{24}$$

By introducing a transit probability for the transition from y_i to y_{i+1}, it can be shown that (22) is a special case of (1).

Computer programming

The mathematical approach involving differential equations to evaluate labelling curves has been chosen, because of its flexibility, enabling some useful generalization to be made. For example, the program permits LI, PLM and CL curves for epidermis in steady state to be evaluated. It is comparable with the programs described by others for the analysis of PLM-curves (Barrett, 1966; MacDonald, 1970; Steel & Hanes, 1971; Takahaski, Hogg & Mendelsohn, 1971; Brockwell, Trucco & Fry, 1972; Gilbert, 1972; Valleron, Mary & Frindel, 1973; Hartmann *et al.*, 1975). By using an optimization procedure it is possible to obtain cell cycle and phase times with their variances, as can be also done using the existing programs. More importantly, the program here described can analyse non-homogeneous populations. This cannot be done by the earlier programs. For any given heterogeneous situations theoretical curves can be generated for the three types of experiment and the cell cycle parameters can be estimated. The computer program can also be used to consider experiments in non-steady state situations. However, here the initial conditions and the nature of the distributions must be known or approximated.

Finally, additional complications can be easily considered, e.g. the influence of circadian rhythms are important in many tissues. In this case only the experimentally known characteristics of the diurnal oscillations of the cell phase times need be considered. This application will be described in more detail elsewhere.

The program (written in FORTRAN) available at present only at the University of Cologne, will soon be available on request

Definition of cell kinetic parameters

Here we consider only the steady state situation, where the sum of the labelled and unlabelled cells is constant. This is described by $Y_C = A, T_1, T_2, T_3, P$ in equation (21). However, since we cannot measure these compartments separately, the corresponding total cell number is required.

$$N = A + T_1 + T_2 + T_3 + P + L \tag{25}$$

where N is the total cell number in the layer and L is the number of 'clear' cells (Langerhans, Merkel, indeterminate and pigment cells), which are assumed to be 15% of N (Allen & Potten, 1974). N_S and N_M would be the corresponding cell numbers in S and M. It is assumed that L cells do not contribute to N_S and N_M since they have a very slow turnover (Schellander & Wolff, 1967; Wolff, 1972; MacKenzie, 1975). For the labelled cells we define similarly

$$N^+(t) = A^+(t) + T_1^+(t) + T_2^+(t) + T_3^+(t) + P^+(t) \tag{26}$$

as the total number of labelled cells in the layer and $N_S^+(t)$ and $N_M^+(t)$ as the corresponding numbers of labelled cells in all S and M phases, again assuming that the clear cells do not label. In this notation we can easily find the relationship between theoretical and experimental results: for the *labelling index curves* $LI(t)(\%)$:

$$LI(t) = \frac{N^+(t)}{N} \times 100$$

$$= \frac{\text{number of all labelled cells in all compartments after flash labelling}}{\text{total number of cells}} \times 100 \tag{27}$$

for the *continuous labelling index* $CL(t)(\%)$:

$$CL(t) = \int_0^t \frac{N^+(t')\,dt'}{N} \times 100$$

$$= \frac{\text{number of labelled cells after continuous labelling}}{\text{total number of cells}} \times 100 \tag{28}$$

for the *curves of the percentage of labelled mitosis* $PLM(t)$:

$$PLM(t) = \frac{N_M^+(t) \times 100}{N_M} = \frac{\text{number of labelled cells in mitosis}}{\text{total number of mitotic cells}} \times 100 \tag{29}$$

for the *proliferative fraction* PF:

$$PF = \frac{A + T_1 + T_2 + T_3}{N} = \frac{\text{number of all proliferating cells}}{\text{total number of cells}} \tag{30}$$

for the *clonogenic fraction* CF (assuming that only stem cells (A) are clonogenic):

$$CF = \frac{A}{N} = \frac{\text{number of stem cells}}{\text{total cell number}} \tag{31}$$

(The reciprocal value of CF represents the number of cells per EPU assuming 1 stem cell per EPU.)
For the *relative number of newly formed cells per day*, NC:

$$NC = \int_0^{24\,hr} \frac{\lambda p\, P dt}{N} = \frac{\text{number of cells leaving the layer per day}}{\text{total cell number}} \tag{32}$$

for the *average cell cycle time* $\bar{T}_C$:

$$\bar{T}_C = \frac{A T_C^A + T_1 T_C^{T_1} + T_2 T_C^{T_2} + T_3 T_C^{T_3}}{A + T_1 + T_2 + T_3} = \text{sum of the weighted cell cycle times of all proliferative compartments} \tag{33}$$

for the *average S-phase time* $\bar{T}_S$:

$$\bar{T}_S = \frac{A_S T_S^A + T_{1S} T_S^{T_1} + T_{2S} T_S^{T_2} + T_{3S} T_S^{T_3}}{N_S} = \text{sum of the weighted S-phase times of all proliferative compartments} \tag{34}$$

for the *basal layer transit time* T_{BL}:

$$T_{BL} = T_C^{T_1} + T_C^{T_2} + T_C^{T_3} + T_P = \text{sum of the transit times through all compartments in the basal layer after leaving}$$
$$\text{the stem cell compartment}$$

(35)

The relative number of cells which are labelled immediately after flash labelling (LI_0) *can be calculated as:*

$$LI_0 = LI(O) = \frac{N_S}{N} = \frac{\text{number of cells in S-phase at time zero}}{\text{total cell number}}$$

(36)

We can link this LI_0 with the average S-phase and cycle times by the familiar formula:

$$LI_0 = f \cdot \frac{\bar{T}_S}{\bar{T}_C} \qquad \text{where } f = f_1 \cdot f_2 \cdot f_3$$

(37)

using the *correction factor f* which can be subdivided into the three parts

$$f_1 = \frac{\bar{T}_C \cdot N_S}{\bar{T}_S \cdot (N - P - L)}$$

(38)

f_1 represents the inhomogeneity in S-phase and cell cycle times. If the ratio T_S/T_C is equal in all proliferative compartments then $f_1 = 1$.

$$f_2 = (N - P - L)/(N - L)$$

(39)

f_2 represents the influence exerted by the presence of post-mitotic P cells in the layer and since it is impossible to distinguish between loss from P or G_1 this factor is analogous to the factor attributable to the exponential age distribution for G_1 discussed elsewhere (Appleton, Wright & Dyson, 1977; Duffil, Wright & Shuster, 1976). It becomes 1 when all mitoses are at right angles to the basement membrane (e.g. model 1).

$$f_3 = (N - L)/N$$

(40)

f_3 represents the influence of the presence of non-keratinocytes, i.e. clear cells (L), which in mouse epidermis amount to 15% of the total basal cells. This could be taken as the growth fraction (GF). If no clear cells exist (L = 0), then $f_3 = 1$.

The proliferative fraction PF can be calculated from f_2 and f_3

$$PF = f_2 \cdot f_3.$$

(41)

Theoretical model results

The mathematical approaches described above can now be considered for each of the models shown in Fig. 1 and related to the experimental results illustrated in Figs 2–6. The mathematical models will be considered at two levels (1) *the idealized situation* without statistical variability (2) *the realistic situation* where statistical variation on the various cellular parameters is considered (using an arbitrary coefficient of variation of about 10% for all cycle times: larger coefficient of variation produce stronger dampening effects).

LI experiments

Idealized situation

The initial LI_0 represents the relative number of labelled cells in all compartments [equation (36)]. In model 1 the LI would remain constant with time. For models 2–5, after the minimum $T_{G_1} + T_M$, the labelled cells start dividing, and their numbers double after the maximum of $T_{G_1} + T_M + T_S$, i.e. at about 15–25 hr in our examples. If there is a delay in loss from the P compartment a plateau would be found in the LI. If cells are lost from P soon after coming into this compartment, then a decrease in LI would occur, thus generating a peak. If the half-life is short (compared with the shortest cell cycle time), the LI curve will decrease to a minimum which represents the relative number of labelled cells in all compartments except P. If $T_{\frac{1}{2}}$ of P is longer then a residuum of P cells may occur at the minimum in the LI curves (e.g. in Figs 7–9).

One cell cycle time after the beginning of the experiment the labelled cells will divide again, giving a second peak in both LI and PLM experiments. If the cells in the last transit compartment divide then labelled cells will again enter P and then will be lost from it as before (Figs 7 and 8). However, if the earlier cells only divide, this results in a plateau in the LI curves (Fig. 9).

The principle for construction of these LI curves from the fraction of labelled cells in the various compartment is simple (Fig. 8).

The development of the peak in LI depends on only two factors: T_C and T_S. If all T_C values are equal, but T_S increases with increasing transit generation, the peaks decrease in size with time. The opposite occurs if T_S decreases from the stem cells to the last transit compartment. If T_S is equal in all compartments then the peaks are

equal in height (Fig. 7). In this situation the peaks decrease in size if T_C decreases from A to T compartments and vice versa. Clearly, if both T_C and T_S vary in the different compartments, the picture is more complicated.

The number of peaks, their spacing and heights depends not only on the type of model considered (i.e. the number of compartments) but also on cell cycle phase differences. As can be seen from the legends to Figs 7 and 9, different models can produce the same LI curves.

Realistic situation

The statistical spread of the phase times indicates that the first labelled cells divide earlier and the last divide later than in the idealized case. This leads to a slight broadening of the first LI peak with the maximum occurring about 3 hr later than in the idealized case. The effects are greater on the later peaks.

Eventually the LI reaches a near constant value which is determined by T_S in the proliferative compartments and the size of the post-mitotic compartment P (which is itself determined by its half-life $T_{\frac{1}{2}}$). Since T_3 is the last proliferative compartment and since $T_S^{T_3}$ determines the initial but T_S^A the final number of labelled cells in T_3, it is the ratio of the T_S in the last proliferative compartment (T_3) and the stem cell compartment (A) that have the greatest influence on the final LI. In Fig. 8 the ratio of $T_S^A/T_S^{T_3}$ equals 0.4 and the corresponding LI ratio is 0.7.

PLM-curves

Idealized situation

The first peak in the PLM begins after the minimum T_{G_2} and ends after the maximum of $T_{G_2} + T_M + T_S$. If these phase lengths are equal in all the proliferating compartments a maximum of 100% labelled cells is obtained with a half-width of T_S (Fig. 7). If T_S varies within the various subpopulations the width of the peak is determined by the minimum T_S in the upper part and the maximum T_S in the lower part of the peak (Figs 8 and 9).

The timing of the subsequent peaks is determined by T_C. If all proliferative cells have the same average T_C then the peaks will be equidistant (with an interval T_C) and the maxima will reach 100% (Figs 7 and 8).

If T_C varies within the various subpopulations, peaks of differing shapes and sizes will occur at different intervals (in the case where all of the larger T_C are integer multiples of the smallest T_C, the interval between peaks may be regular). The height of the peaks depends on the ratios of T_M within the subpopulations. The maxima may decrease with time, or they also may alternate (Fig. 9). The width of the peaks is determined only by T_S. If these differ then the influence of T_S^A increases from one peak to the next and eventually it determines the width (Figs 8 and 10).

Realistic situation

Since T_S determines the width the addition of variation in T_S means that the first peak may reach 100% in some cases but not in all cases (Figs 8 and 9). The later peaks are strongly damped by inclusion of statistical variation in cycle phase lengths, e.g. a peak may reach 100% without variation but only reaches 50% or less when variation is included (Fig. 7).

If T_C differs in each proliferative subpopulation some second peaks might be expected but the dampening effects would soon result in a merging of successive peaks. Thus, discrete peaks might only be expected if T_C varies by near integer factors.

CL-curves

Here the influence of statistical variation in cell cycle phase lengths is less important and can be ignored.

The CL-curves show a slow increase during $T_{G_2} + T_M$ due to influx into S. After this the labelled cells themselves divide and rate of increase in CL is enhanced. The CL is also enhanced by the continual loss of P cells with time and initially these are unlabelled.

If T_C is equal in all subpopulations there is a linear increase in labelling in all proliferative compartments and all cells except clear cells will be labelled after $T_{G_2} + T_M + T_{G_1}$. The result is a CL-curve which increases nearly linearly over the first two thirds of T_C and then continues increasing more gradually to reach 85% after about T_C (Figs 7 and 8) assuming 15% non-replacing clear cells.

If different T_C values exist, the situation is slightly more complicated with a more distinct biphasic increase (e.g. Fig. 9). After a time equivalent to the minimum T_C (100 hr in Fig. 9) all cells of the corresponding compartments will be labelled and the curve will increase more slowly after this, reaching 85% after the maximum T_C 200 hr in Fig. 9).

REFERENCES

ALLEN, T.D. & POTTEN, C.S. (1974) Fine structural identification and organization of the epidermal proliferative unit. *J. cell Sci.* 15, 291.

APPLETON, D.R., WRIGHT, N. & DYSON, P. (1977) The age distribution of cells in stratified squamous epithelium *J. theor. Biol.* 65, 769.

BARRETT, J.C. (1966) A mathematical model of the mitotic cycle and its application to the interpretation of percentage labelled mitosis data. *J. nat. Cancer Inst.* **37**, 443.

BROCKWELL, P.J., TRUCCO, E. & FRY, R.J.M. (1972) The determination of cell-cycle parameters from measurements of the fraction of labelled mitoses. *Bull. Math. Biophys.* **34**, 1.

DUFFIL, M., WRIGHT, N. & SHUSTER, S. (1976) The cell proliferation kinetics of psoriasis examined by three in vivo techniques. *Br. J. Derm.* **94**, 355.

GILBERT, C.W. (1972) The labelled mitoses curve and the estimation of the parameters of the cell cycle. *Cell Tissue Kinet.* **5**, 53.

HARTMANN, N.R., GILBERT, C.W., JANSSON, B., MACDONALD, P.D.M., STEEL, G.G. & VALLERON, A.J. (1975) A comparison of computer methods for the analysis of fraction labelled mitosis curves. *Cell Tissue Kinet.* **8**, 119.

MACDONALD, P.D.M. (1970) Statistical inference from the fraction labelled mitoses curve. *Biometrika*, **57**, 489.

MACKENZIE, I.C. (1975) Labelling of murine epidermal Langerhans cells with ^{3}H-thymidine. *Am. J. Anat.* **127**, 000.

SCHELLANDER, F. & WOLFF, K. (1967) Zur Autoradiographischen Markierung von Langerhandzellen mit ^{3}H-thymidin. *Arch. Klin. exp. Derm.* **230**, 140.

STEEL, G.G. & HANES, S. (1971) The technique of labelled mitoses: Analyses by automatic curve-fitting. *Cell Tissue Kinet.* **4**, 93.

TAKAHASHI, M., HOGG, D.G. & MENDELSOHN, M.L. (1971) The automatic analysis of FLM curves. *Cell Tissue Kinet.* **4**, 505.

VALLERON, A.-J., MARY, J.Y. & FRINDEL, E. (1973) Methode d'analse sur ordinateur des corbes de mitoses marquees. *Biomedicine*, **18**, 118.

WOLFF, K. (1972) The Langerhans cell. *Current Problems Der.* **4**, 79.